

## The ptychoid defensive mechanism in Euphthiracaroidea (Acari: Oribatida): A comparison of exoskeletal elements

Sebastian Schmelzle<sup>1\*</sup>, Lukas Helfen<sup>2</sup>, Roy A. Norton<sup>3</sup> & Michael Heethoff<sup>1</sup>

<sup>1</sup> Universität Tübingen, Zoologisches Institut, Abteilung Evolutionsbiologie der Invertebraten, Auf der Morgenstelle 28E, 72076 Tübingen, Germany; e-mail: sebastianschmelzle@gmail.com

<sup>2</sup> Institute for Synchrotron Radiation, ANKA, Forschungszentrum Karlsruhe, 76021 Karlsruhe, Germany

<sup>3</sup> State University of New York, College of Environmental Science and Forestry, 1 Forestry Drive, Syracuse NY 13210, USA

\* Corresponding author

### Abstract

Ptychoidity is a mechanical defensive mechanism of some groups of oribatid mites, in which the legs and coxisternum can be completely retracted into the idiosoma and the prodorsum acts as a seal to the encapsulated animal. Here, we use two microscopical techniques, scanning electron microscopy and synchrotron X-ray microtomography, to compare exoskeletal features of two species of ptychoid oribatid mites. *Oribotritia banksi* and *Rhysotritia ardua* both belong to the superfamily Euphthiracaroidea and are analysed here in direct comparison to *Euphthiracarus cooki*, for which the functional morphology has already been described. *Rhysotritia ardua* and *E. cooki* – both members of Euphthiracaridae – are similar in most skeletal features that relate to ptychoidity, but differ in the size of their postanal apodemes. *Oribotritia banksi* – a member of Oribotritiidae – differs from the former two in some well-known features, including the retention of articulations between components of the ventral plates (compared to fused, holovalental plates in Euphthiracaridae), and the absence of interlocking triangles that are associated with the pre- and postanal apodemes in Euphthiracaridae. Our study uncovered two internal skeletal differences in the prodorsum that relate to muscle attachment surfaces: compared to *E. cooki* and *R. ardua*, *O. banksi* lacks the sagittal apodeme and has a distinctly smaller manubrium, but only the latter functions in ptychoidity.

**Keywords:** Synchrotron-X-Ray-Microtomography, *Euphthiracarus cooki*, *Rhysotritia ardua*, *Oribotritia banksi*

### Zusammenfassung

Ptychoidity ist ein bei einigen Gruppen der Oribatida verbreiteter mechanischer Defensivmechanismus, bei dem die Beine und das Coxisternum komplett in das Idiosoma eingezogen werden können und das Prodorsum dann als Verschlusskappe des eingekapselten Tieres fungiert. Wir verwenden hier zwei verschiedene mikroskopische Techniken, Rasterelektronenmikroskopie und Synchrotron-Röntgen-Mikrotomographie, um die exoskeletalen Anpassungen zweier Gattungen ptychoider Oribatida zu vergleichen. *Oribotritia banksi* und *Rhysotritia ardua* gehören beide zu der Gruppe der Euphthiracaroidea und werden im direkten Vergleich mit *Euphthiracarus cooki*, bei dem die funktionelle Morphologie schon beschrieben ist, untersucht. *Rhysotritia ardua* und *E. cooki* – beide zur Familie der

Euphthiracaridae gehörend – besitzen in den meisten skeletalen Merkmalen die in Verbindung mit Ptychoidie stehen große Ähnlichkeit, weichen aber in der Größe des postanalen Apodems voneinander ab. *Oribotritia banksi* – zur Familie der Oribotritiidae gehörend – unterscheidet sich von den beiden in einigen Merkmalen: zwischen den Komponenten der ventralen Platten befinden sich Gelenke, welche bei den verschmolzenen holozentralen Platten der Euphthiracaridae fehlen; weiterhin fehlen den Euphthiracaridae die den prä- und postanal Apodemen zugehörigen Verbindungsdreiecke. Unsere Untersuchung deckt zwei interne skeletale Unterschiede im Prodorsum auf, die sich auf Muskelansatzstellen beziehen: im Vergleich zu *E. cooki* und *R. ardua* fehlt *O. banksi* das sagittale Apodem und diese Art besitzt ein deutlich kleineres Manubrium, wobei nur letzteres bei der Ptychoidie eine Rolle spielt.

## 1. Introduction

Oribatid mites are a speciose group of mainly soil-dwelling microarthropods. About 9000 – 10 000 species have been described, but estimates of true diversity range from 50 000 – 100 000 (Travé et al. 1996, Schatz 2002, Subías 2004). Oribatid mites have an unusual feeding behaviour among the Chelicerata: they consume particulate instead of fluid food. The lower quality of the resources and a lower digestive efficiency result in slow growth, a relatively long generation time and low reproductive potential, which requires a long adult life-span (Norton 1994). Hence, another characteristic of the Oribatida is their diverse strategies and adaptations for predator defence. Some relate to chemical defences associated with opisthotal oil glands, which produce a variety of hydrocarbons, terpenes, aromatic compounds and alkaloids that are demonstrated or thought to relate to alarm pheromones, antimicrobial activity or predator repulsion (e.g. Shimano et al. 2002, Raspotnig 2006, Saporito et al. 2007). Mechanical defences include modified body setae, which can variously result in a hedgehog-like appearance or scale-like covering of the body. Cuticular hardening by sclerotisation or mineralisation is widespread. The latter can involve deposition of calcium carbonate, calcium phosphate or calcium oxalate (Norton & Behan-Pelletier 1991; Alberti et al. 2001). If the cuticle is hardened, protection of soft articulations can be achieved through the formation of overhanging tecta (Grandjean 1934).

A special defensive strategy is seen in the ptychoid body form, which involves several exoskeletal adaptations. The walking legs and the coxisternum can be completely retracted into the idiosoma, after which the prodorsum seals the secondary cavity to create an encapsulated state, in which the animals are firmly closed and appear seed-like (Figs 1B, D). In the active extended state, they look and move much like mites with a dichoid body form (Figs 1A, C). As a defensive behaviour, a few species exhibit a combination of ptychoidy with an escape jump (Wauthy et al. 1998). The ptychoid body form presumably has evolved at least three times (Sanders & Norton 2004). Two families of the Enarthronota, Protoplophoridae and Mesoplophoridae, have developed ptychoidy independently (Grandjean 1969, Norton 1984, Norton 2001). All other ptychoid families are members of Ptyctima (Mixonomata), including the two superfamilies Phthiracaroidae and Euphthiracaroidae (Grandjean 1954, Grandjean 1967, Balogh & Balogh 1992).

With such convergence on a similar set of adaptations, there is a strong possibility that mechanical problems were solved in different ways, but to demonstrate this requires good

knowledge of each group. Here, we present a comparative study of the exoskeletal features associated with ptychoidy in two species of Euphthiracaroida, *Oribotritia banksi* Oudemans and *Rhysotritia ardua* Koch, and compare the results with the morphology of *Euphthiracarus cooki* (Sanders & Norton 2004). General features of these mites were described by Märkel & Meyer (1959; see Mahunka 1990 and Haumann 1991 for discussions of their systematics and evolution). Since exoskeletal adaptations to ptychoidy are found in different parts of the body, we examine five distinct regions: the prodorsum, the opisthosomal venter, the notogaster, the podosoma and the subcapitulum.

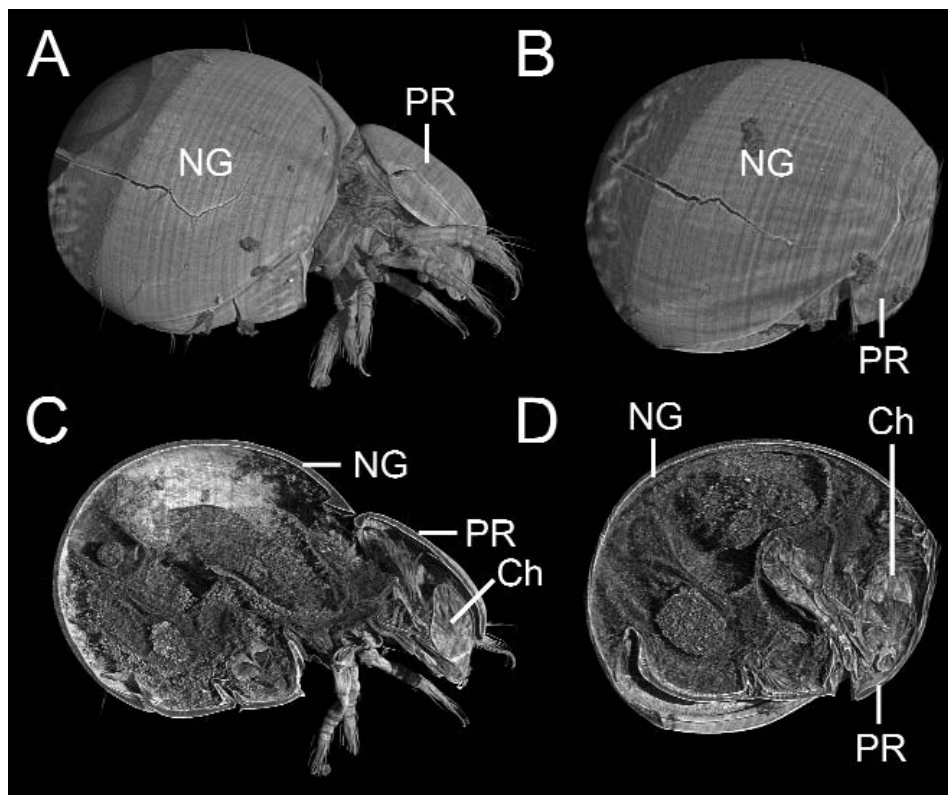


Fig. 1 Renditions of synchrotron-X-ray-microtomography data of *Phthiracarus globulosus* in extended (A, C) and encapsulated state (B, D). A: Extended animal showing a nearly dichoid body form. B: Encapsulated animal showing a seed-like appearance. C: Virtual sagittal section showing the positions of the legs and the organs in extended state. D: Same, but in encapsulated state. Ch: chelicera; NG: notogaster; PR: prodorsum.

### 1.1. Prodorsum

The prodorsum acts as an operculum-like seal for the encapsulated animal. Thus, there are adaptations that provide suitable origins or insertions for the musculature that is responsible for entpychosis (the enclosing of the animal) and ecptychosis (the opening of the animal). Additionally there are adaptations that help fit the prodorsum perfectly onto the opisthosoma. The distal part of the prodorsum is the solid rostral limb that merges with the rostromphragma (Grandjean 1939 called it the ‘cloison rostral’) which, in turn, merges with the tegulum, the soft cuticular frame around the chelicerae (Sanders & Norton 2004). Attachment points for musculature include the manubrium, a process at the posterior laterovenral edge of the prodorsum; the inferior retractor process at the lateral interior wall; and the sagittal apodeme, which is located medially on the posterior wall of the prodorsum. Two types of structures interact with nearby body regions to ensure that the prodorsum aligns properly during entpychosis. One is the bothridial scale, a process located laterodorsally near the bothridial seta, or sensillus. The other includes two or three lateral, longitudinal carinae. The dorsal and sometimes middle carinae originate at the bothridial scale, while the ventral carina, near the prodorsal border, originates in the nuchal region. All end near the rostral notch, a gentle depression of the ventral outline of the prodorsum.

### 1.2. Opisthosomal venter

The opisthosomal venter consists of a number of elongated paired plates that comprise: the plicature plates (sclerotised ventral plicature band of Grandjean 1933, 1967); the fused aggenital and adanal plates; and genital and anal plates that may be independent (in Oribotritiidae) or may be fused with each other and with the former to form a holovenral plate (in Euphthiracaridae; Norton et al. 2003). The holovenral plate occurs only in Euphthiracaridae. At the anterior (podosomal) edge, these plates turn vertically to form the phragma, with the pair connected through the phragmatal bridge; since they lack muscle attachments, these structures are considered solely structural, adding transverse stability to the venter (Sanders & Norton 2004). Anteriorly, the ventral plates can form a carina, which accommodates to the rostrum and thereby helps in completely sealing the encapsulated animal. In Euphthiracaridae, between the genital (about at the middle of the holovenral plates) and anal atrium (at the posterior end of the holovenral plates) an inward facing sclerotised structure, the prominence of the preanal apodeme, connects the two holovenral plates together. At its ventral margin is the anterior interlocking triangle, which is formed by interdigitating corrugations of the opposing plates. At the posterior end of the anal atrium, a similar postanal apodeme and interlocking triangle may be present.

### 1.3. Notogaster

The notogaster is heavily mineralised and therefore very rigid. For building up hemocoel pressure, the notogaster can be flexed inward so that its opening at the ventral end lessens. This is accomplished by a series of muscles that span the folds of the venter, which when contracted decreases the angle between the plates, thereby flexing the notogaster. This increases the hemocoel pressure for the ecptychosis, the opening of the enclosed animal (Sanders & Norton 2004). The notogastral fissure at the posterior end of the notogaster ensures that – even at that especially firm location – a certain level of flexure is possible.

Anterior adaptations allow the prodorsum to fit perfectly onto the notogaster at entychosis. The notogastral collar at the anterior border of the notogaster is divided into two parts, the pronotal tectum and the lateral anterior tectum. In the encapsulated state the lateral anterior tectum fits perfectly to the dorsal carina of the prodorsum and the pronotal tectum covers the articulation between notogaster and prodorsum. Between the pronotal tectum and the lateral anterior tectum is an emargination, the tectonotal notch. This notch comprises the scale receptacle that anchors the bothridial scale of the prodorsum when encapsulation is complete, and is supposed to add precision to the movement during entychosis (Walker 1965).

#### 1.4. Podosoma

The podosoma is very soft, except for the epimeres, with three different lines or furrows. The abjugal line marks the anterior boundary of the podosoma to the epiprosoma (consisting of prodorsum, chelicerae and subcapitulum) and the disjugal line marks the posterior boundary of the podosoma and the idiosoma. The podosoma itself is divided by the sejugal line, which runs between the leg bearing segments two and three, separating the proterosoma and hysterosoma. The soft podosoma with its different articulating lines is one of the adaptations that enable entychosis. The articulation between subcapitulum and epimeres 1 is V-shaped, the circumcapitular furrow. The articulation between epimeres 2 and 3 comprises the ventrosejugal furrow. Epimeres 1 are the largest and are undivided, but other epimeres are subdivided by a soft median furrow of different widths (Sanders & Norton 2004). In the centre of the coxisternum (all epimeres, collectively) is a large area of membrane, the coxisternal umbilicus. It functions as a reservoir that holds enough membrane for the folding and reorienting of the epimeres during entychosis (Sanders & Norton 2004).

#### 1.5. Subcapitulum

At least in *Euphthiracarus cooki*, the subcapitular adaptations for ptychoidy include a prominent capitular apodeme and equally prominent projection of the mentum, as well as the fusion of the taenidiophore part of supracoxal sclerite 1 to the subcapitulum. In most oribatid mites, the capitular apodeme protrudes into the interior as a narrow sclerotised shelf. In Ptyctima, the capitular apodeme can instead be a large triangular, flat process. The capitular apodeme is reinforced at its margins by a lemniscus (Sanders & Norton 2004). Normally in oribatid mites, the taenidiophore projects from the expanded dorsal border of supracoxal sclerite 1 and acts as a dicondylic articulation between the subcapitulum and the podosoma.

## 2. Materials and methods

### 2.1. Specimens

Living specimens of *Oribotritia banksi* were collected by R. A. Norton from forest litter in the Otter Creek Wilderness, West Virginia, USA, in May 2005 and extracted the following year after prolonged storage. Specimens of *Rhysotritia ardua* were collected by R. A. Norton in Lafayette, New York, USA, in November 2006 and extracted immediately.

## 2.2. Sample preparation

Live specimens were killed and fixed in 1 % glutaraldehyde for 60 hours and then stored in 70 % ethanol for shipping. Afterwards the specimens were dehydrated stepwise in an increasing ethanol series of 70 %, 80 %, 90 %, 95 %, and 100 %, with each step being repeated three times for 10 minutes. The samples were stored overnight in fresh 100 % ethanol and then critical-point dried in CO<sub>2</sub> (CPD 020, Balzers).

## 2.3. Imaging techniques

### 2.3.1. Scanning electron microscopy

Dried specimens were sputter-coated with a 20-nm thick layer of a gold-palladium mixture. Micrographs were taken on a Cambridge Stereoscan 250 Mk2 scanning electron microscope at 20 keV.

### 2.3.2. Synchrotron-X-Ray-Microtomography

Dried specimens were super-glued to the tip of a plastic pin (1.2 cm long; 3.0 mm in diameter) and mounted onto a goniometer head. Microtomography scans were carried out at the European Synchrotron Radiation Facility (ESRF) in Grenoble at beamline ID19 (experiment SC-2127). For each scan, a multitude (typically 1500) of x-ray radiographs (with a resolution of up to 2048 x 2048 pixels) with an effective pixel size of 0.7 µm were acquired at an x-ray energy of 20.5 keV and an object-detector distance of 20 mm, making use of the coherence properties of the incident x-ray beam to obtain edge-enhancing phase contrast. For further information on the technique, see Betz et al. (2007). The tomographic voxel-data were visualised with VGStudio MAX (Volume Graphics, Heidelberg, Germany) and segmented in amira™ (Mercury Computer Systems Inc., Chelmsford, Massachusetts).

## 3. Results

### 3.1. Prodorsum

The inner texture of the prodorsum itself is uniform in *Rhysotritia ardua* (Fig. 2B), but rough-textured in *Oribotritia banksi* (Fig. 2A). In *R. ardua* the differentiation between the solid, distal rostral limb (rl) and the rostrum (rp) at point y and between the rostrum and the tegulum (teg) at point x (Fig. 3B) is distinct. In contrast, at least the sum-along-ray picture (a virtual x-ray rendering of the 3D data) of the prodorsum of *O. banksi* (Fig. 3A) shows no clear differentiation, although it is visible in the original synchrotron micrographs. The manubrium differs between the species. In *O. banksi* it is a short stump (Fig. 3C, mn), with a broad and very robust base. In *R. ardua*, it is longer, with the base being relatively smaller (Fig. 3D, mn). The inferior retractor process appears similar in both species, though it is slightly shallower in *O. banksi* (Fig. 3E, irp). The sagittal apodeme in *R. ardua* is well developed (Fig. 3F, sa), but in *O. banksi* there is no evidence of it at all. The bothridial scale of *O. banksi* (Figs 4C, E; bs) is slightly more rounded with a small distal dent, compared to the relatively square one of *R. ardua* (Figs 4D, F; bs). The sensillus of the two species is very different: in *O. banksi* it tapers distally (Fig. 4E, ss), while it splits into many small branches in *R. ardua* (Fig. 4F, ss). In both species, the bothridium is ventral to the bothridial

scale, so that at emptychosis it is squashed into the articulation (Figs 2A – D). Around the internal part of the bothridium is a system of chambers. Laterally on the prodorsum there are two carinae – dorsal and ventral – in both animals (Figs 5A, B; Figs 3C, D). They end near the rostral notch, which is more distinct in *R. ardua* (Fig. 5A, rn) than in *O. banksi* (Fig. 3B).

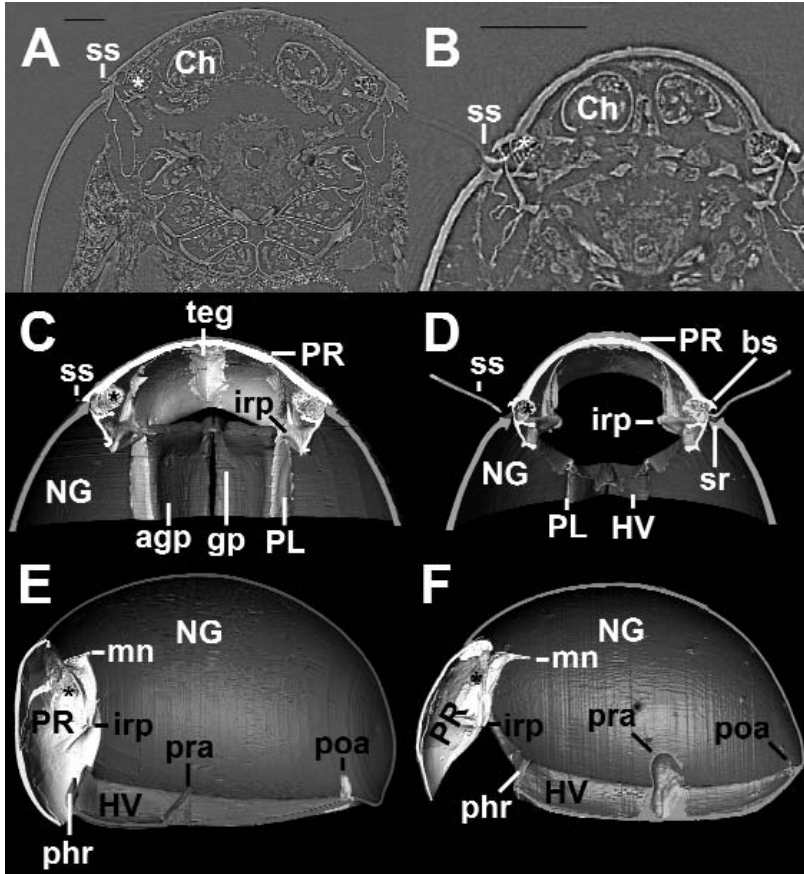


Fig. 2 Virtual transverse sections of synchrotron-X-ray-microtomography data (A, B) and virtual sections of synchrotron-X-ray-microtomography data of 3-D models (C, D dorsal view; E, F lateral view). A: *O. banksi*. Detail in the region of the bothridium. A: *R. ardua*, same. C: *O. banksi*, same as in A. D: *R. ardua*, same. E: *O. banksi*, prominence of preanal and postanal apodeme are clearly shown, also the manubrium. The aggenital and genital plate are not distinguishable on this picture; therefore they are combined as the genital region (gr). The adanal and anal plate are not distinguishable on this picture; therefore they are combined as the anal region (ar). F: *R. ardua*, same. The three-dimensional modelling (segmentation) of the tegulum on C – F is not completed. agp: aggenital plate; ar: anal region; bs: bothridial scale; Ch: chelicera; gp: genital plate; gr: genital region; HV: holoventral plates; irp: inferior retractor process; mn: manubrium; NG: notogaster; phr: phragma of holoventral plate; PL: plicature plates; poa: postanal apodeme; PR: prodorsum; pra: prominence of preanal apodeme; ss: sensillus; teg: tegulum. Asterisk indicates bothridium.

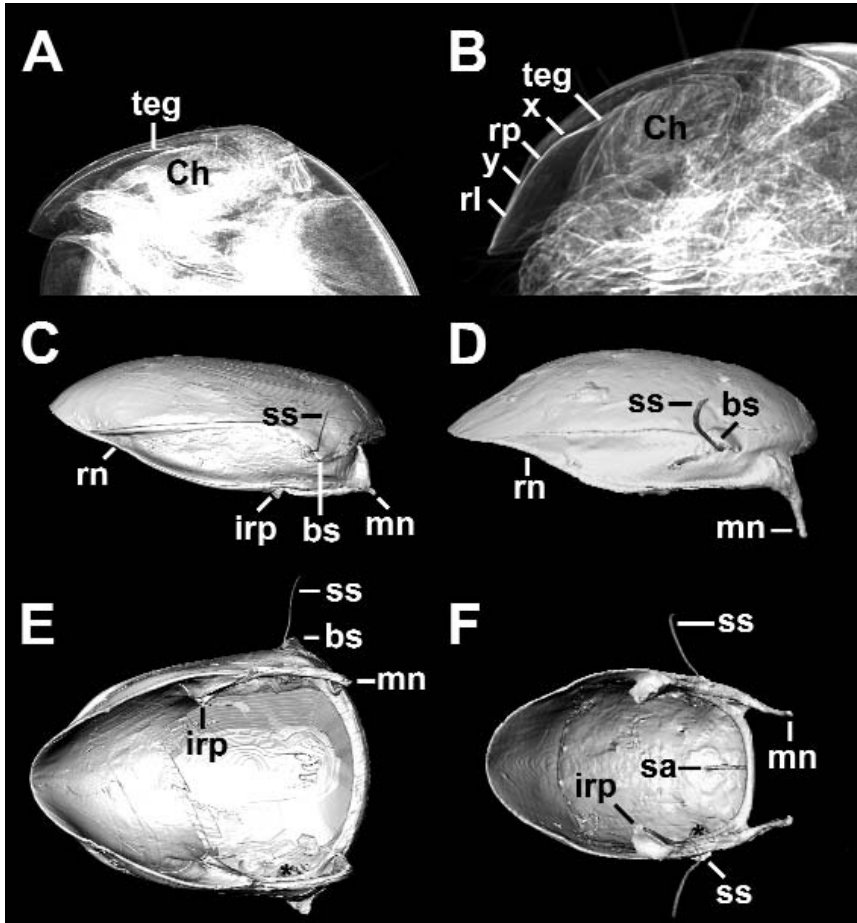


Fig. 3 Lateral view of renderings of the prodorsum with synchrotron-X-ray-microtomography data. a, b; Sum along ray (a rendering option in 'VGStudio Max': a virtual x-ray projection of the 3D data), and 3D models (C, D lateral view; E, F posterior view). A: *O. banksi*. X-ray-like image to illustrate the structure of the prodorsum. B: *R. ardua*, same as in A. C: *O. banksi*, lateral view of prodorsum with short manubrium. D: *R. ardua*, lateral view of prodorsum with long manubrium. E: *O. banksi*. F: *R. ardua*, same as in E. The tegulum in E and F is not shown. bs: bothridial scale; Ch: chelicerae; irp: inferior retractor process; mn: manubrium; PR: prodorsum; rl: rostral limb; rn: rostral notch; rp: rostraphragma; sa: sagittal apodeme; ss: sensillus; teg: tegulum; x, y: proximal and distal limits of rostraphragma. Asterisk indicates bothridium.

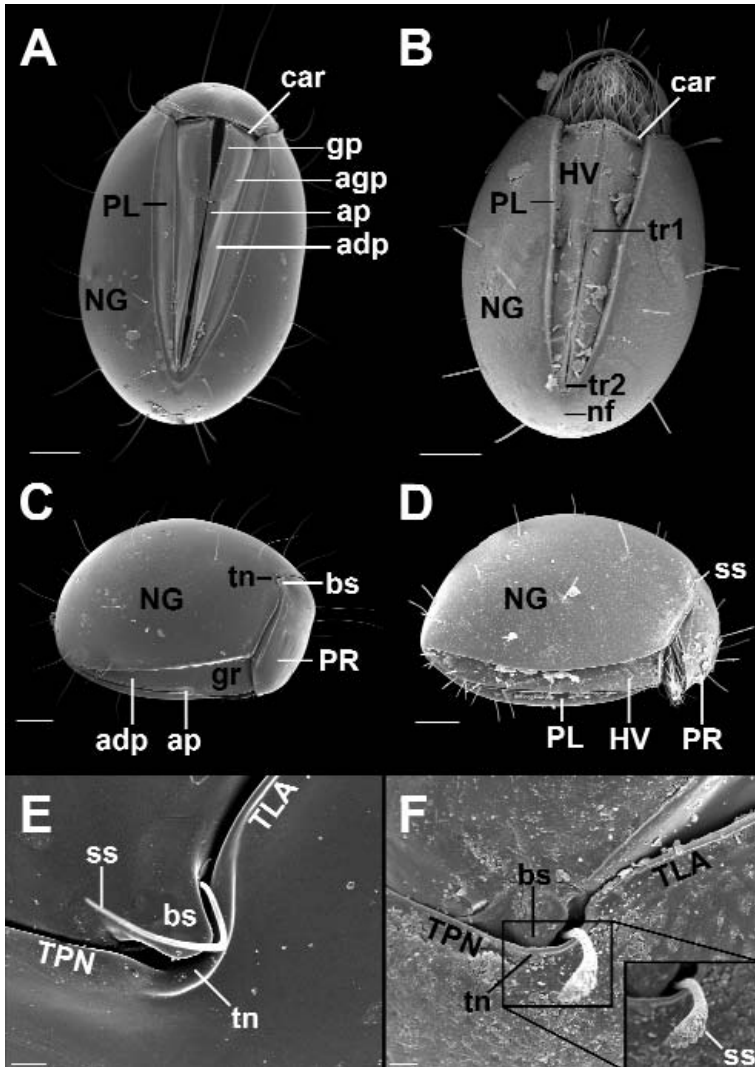


Fig. 4 Scanning electron micrographs. A: *Oribotritia banksi* in nearly encapsulated state, ventral view (scale bar: 200  $\mu\text{m}$ ). B: *Rhysotrititia ardua* in partly encapsulated state, ventral view (scale bar: 100  $\mu\text{m}$ ). C: *O. banksi* in nearly encapsulated state, lateral view. The aggenital and genital plate are not distinguishable in this picture; therefore they are combined as the genital region (gr) (scale bar: 200  $\mu\text{m}$ ). D: *R. ardua* in partly encapsulated state, lateral view (scale bar: 100  $\mu\text{m}$ ). E: Detail of the bothridial scale, the sensillus and the tectonotal notch of *O. banksi* (scale bar: 20  $\mu\text{m}$ ). F: Same as in E, but from *R. ardua* (scale bar: 10  $\mu\text{m}$ ). The frame shows the same area, but with focus on the tip of the sensillus. adp: adanal plate; agp: aggenital plate; ap: anal plate; bs: bothridial scale; car: carina; gp: genital plate; gr: genital region; HV: holovenral plates; nf: notogastral fissure; NG: notogaster; PL: plicature plates; PR: prodorsum; ss: sensillus; TLA: lateral anterior tectum; tn: tectonotal notch; TPN: pronotal tectum; tr1: interlocking triangle one; tr2: interlocking triangle two.

### 3.2. Opisthosomal venter

The plicature plates run paramedian from the anterior margin of the notogaster and fade out to posterior in both species. Those of *R. ardua* (Fig. 4B, PL) are rather narrow, relative to those of *O. banksi* (Fig. 4A, PL). The holovenal plates of *R. ardua* are nearly constant in width except close to the posterior margin (Figs 6F, 4B; HV), whereas the homologous collective plates of *O. banksi* narrow continually, from anterior to posterior (Figs 2E, 4A; HV). Additionally, the holovenal plates, present in *R. ardua*, do not exist in *O. banksi* where the adanal and anal plates as well as the aggenital and genital plates are not fused (Figs 4A, 7A, C). There is no distinct difference between the carina, phragma or phragmatal bridge in *O. banksi* and *R. ardua* (Figs 7A, B; 5C, D). The postanal apodeme in *R. ardua* is extremely small, whilst the prominence of the preanal apodeme is relatively large (Fig. 2F, poa, pra). By contrast, in *O. banksi*, the size of these two apodemes is quite similar (Fig. 2E, poa, pra). The interlocking triangle 1 of *R. ardua* has six interdigitating corrugations (Fig. 6B, tr1), while that of interlocking triangle 2 has four (Fig. 6D, tr2). As in all members of Oribotritiidae, there is no interlocking triangle associated with either apodeme in *O. banksi* (Fig. 6C). Instead, it looks like an overhang of the anterior plate, directed posteriorly.

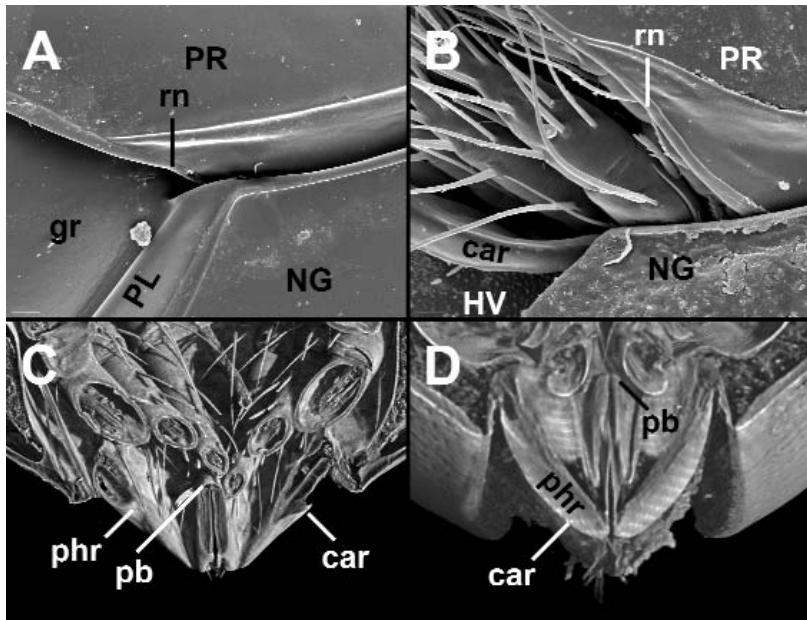


Fig. 5 Scanning electron micrographs, lateral view (A, B) and renderings of transversal sections with synchrotron-X-ray-microtomography data (C, D), frontal view. A: *O. banksi*. Detail of the rostral notch region. The aggenital and genital plate are not distinguishable in this picture; therefore they are combined as the genital region (gr). (scale bar: 20  $\mu$ m). B: Same, but from *R. ardua*. (scale bar: 10  $\mu$ m). C: *O. banksi*. Detail of the anterior region of the ventral plates. Visible is also the connecting phragmatal bridge. D: *R. ardua*, same as in C. car: carina; gr: genital region; HV: holovenal plates; NG: notogaster; pb: phragmatal bridge; phr: phragma of ventral plate; PL: plicature plate; rn: rostral notch.

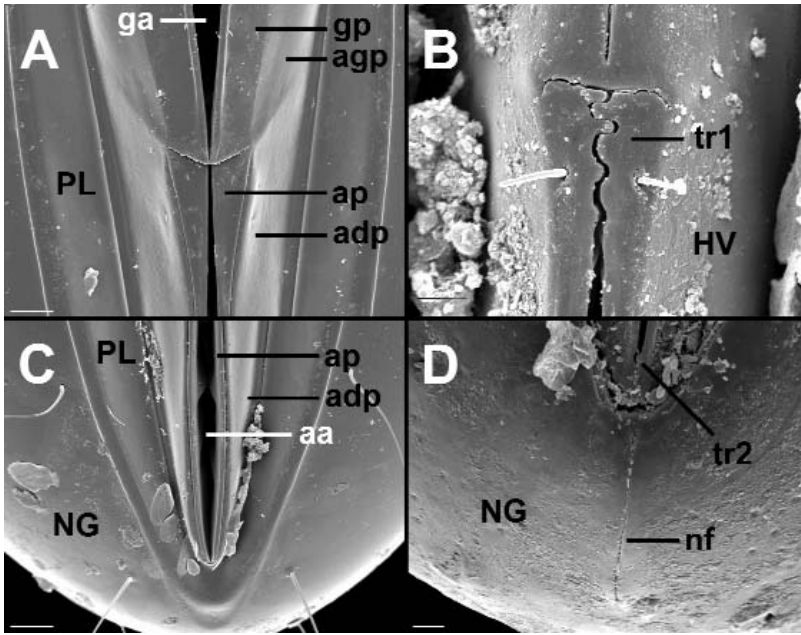


Fig. 6 Scanning electron micrographs, ventral view. A: *O. banksi*. Detail of the region of the interlocking triangle 1 (scale bar: 50  $\mu\text{m}$ ). B: *R. ardua*. Detail of the region of the interlocking triangle 1 (scale bar: 10  $\mu\text{m}$ ). C: *O. banksi*. Detail of the region of the interlocking triangle 2 (scale bar: 50  $\mu\text{m}$ ). D: *R. ardua*. Detail of the region of the interlocking triangle 2 and the notogastral fissure (scale bar: 50  $\mu\text{m}$ ). aa: anal atrium; adp: adanal plate; agp: aggenital plate; ap: anal plate; ga: genital atrium; gp: genital plate; HV: holoventral plates; nf: notogastral fissure; NG: notogaster; PL: plicature plates; tr1: interlocking triangle one; tr2: interlocking triangle two.

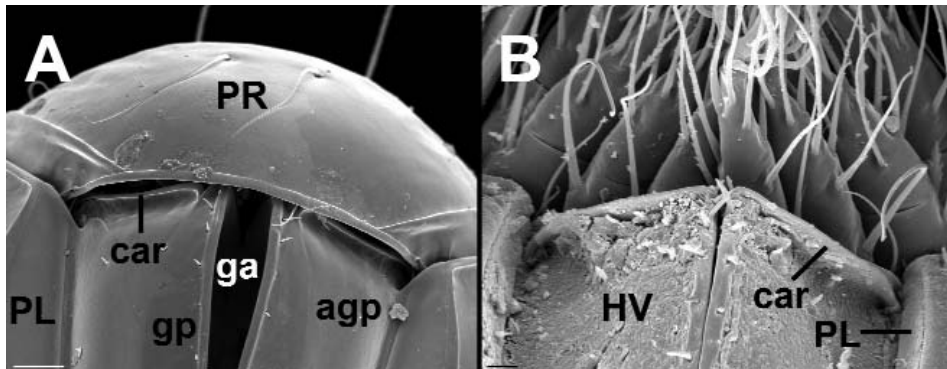


Fig. 7 Scanning electron micrographs. Specimens in nearly encapsulated state, ventral view. The carina is located at the anterior margin of the ventral plates. A: *O. banksi* (scale bar: 50  $\mu\text{m}$ ). B: *R. ardua* (scale bar: 10  $\mu\text{m}$ ). car: carina; ga: genital atrium; HV: holoventral plates; NG: notogaster; PL: plicature plates; PR: Prodorsum.

### 3.3. Notogaster

*Oribotritia banksi* lacks a terminal notogastral fissure (Fig. 6C), but it is present in *R. ardua* (Fig. 6D, nf). The pronotal tectum and the lateral anterior tectum are similar in both species (Figs 4E, F; TPN, TLA). The margin of the tectonotal notch of *R. ardua* is a nearly round, continuous half circle (Fig. 4F; tn), while in *O. banksi* it has a lateral elevation (Figs 4C, E; tn). In *R. ardua*, the scale receptacle is visible as a furrow on the anterior margin of the notogaster (Fig. 2D; sr), but there is no obvious receptacle in *O. banksi* (Fig. 2C).

### 3.4. Podosoma

There is no noticeable difference in the podosoma of *O. banksi* and *R. ardua*. Both species feature the circumcapitular furrow, ventrosejugal furrow, the median furrow and the coxisternal umbilicus.

### 3.5. Subcapitulum

The capitular apodeme and its lemniscus are nearly identical in *O. banksi* and *R. ardua*. The location of the taenidiophore has not yet been discovered.

## 4. Discussion

Grandjean (1969) suggested three exoskeletal characteristics that were necessary prior to the evolution of ptychoidy in any oribatid mite group, and Norton (2001) suggested a fourth. First, the coxisternum must be surrounded only by flexible integument with no direct connection to hard cuticular elements. Second, except for articulations, the opisthosomal cuticle must be hardened. Third, the coxisternum must be articulated and therefore deformable. Fourth, some aspect of structure must be able to accommodate the large internal volume changes associated with leg retraction and extension, and be able to inflate a pliable podosoma hydraulically with sufficient pressure to support ambulatory activity. These traits are present in *Oribotritia banksi* and *Rhysotritia ardua*, but these species differ in some details, which are compared below with those of *Euphthiracarus cooki*, as described by Sanders & Norton (2004).

### 4.1. Prodorsum

The inner texture of the prodorsum is uniform in both *E. cooki* and *R. ardua* but rough-textured in *O. banksi*. The proximal and distal borders of the rostraphragma are distinct in *R. ardua* and *E. cooki*, but not in *O. banksi*. The manubrium is elongated in *E. cooki* and *R. ardua*, but that of *O. banksi* is merely a short stump. The inferior retractor process is similar in all three species. The sagittal apodeme is well developed in *R. ardua* and *E. cooki*, but absent in *O. banksi*. The bothridial scale of *O. banksi* and *E. cooki* is slightly rounder than in *R. ardua*. Only the latter species has a small indentation at its distal margin, which could be a resting place for the sensillus during entpychosis. The sensillus differs in all three species: split into many small branches in *R. ardua*, broadened in *E. cooki*, and tapered in *O. banksi*. In both *O. banksi* and *R. ardua*, the bothridial scale is located dorsally to the sensillus. However, it is located ventrally to it in *E. cooki*, so that it remains free of the articulation at entpychosis. Around the internal part of the bothridium is a system of chambers in all species.

Grandjean (1967) described them as internalised cuticular chambers, which in Euphthiracaridae have short tracheae that are probably respiratory structures.

Lateral on the prodorsum there are two carinae in both *O. banksi* and *R. ardua*, but three carinae (dorsal, medial and ventral) in *E. cooki*. The rostral notch of *E. cooki* is far more distinct than in *R. ardua* or in *O. banksi* (Fig. 3B).

#### 4.2. Opisthosomal venter

*Rhysotritia ardua* and *E. cooki* are very similar in having holovenral plates that taper very little along their length, whereas in *O. banksi*, the various ventral plates are not fused and collectively they gradually taper posteriorly. The former two species share interlocking triangles at the bases of the preanal and postanal apodemes – which are absent from *O. banksi* – although the posterior triangle in *R. ardua* is less conspicuous than that of *E. cooki*. Various authors have mistakenly considered the posterior triangle to be absent from members of *Rhysotritia* and used this as a diagnostic trait (e.g. Märkel & Meyer 1959, Balogh & Balogh 1991). The posterior apodeme in *R. ardua* is also much smaller in vertical dimension than the anterior one, whereas in both *E. cooki* and *O. banksi* the two apodemes are similar in size (Fig. 2E, poa, pra). The anterior carina is similar in all the species.

#### 4.3. Notogaster

At its ventral end, the lateral anterior tectum of *E. cooki* is prolonged into a tooth, but both *R. ardua* and *O. banksi* lack this tooth. Both *R. ardua* and *E. cooki* have the terminal notogastral fissure, but *O. banksi* lacks it. The pronotal tectum and the lateral anterior tectum are similar in all three species. In *O. banksi* and *E. cooki* the tectonotal notch has a lateral elevation, but the margin of the notch in *R. ardua* is a continuous half circle. In both *R. ardua* and *E. cooki* the scale receptacle is present as a furrow on the anterior margin of the notogaster, but a receptacle is not distinctly developed in *O. banksi*.

#### 4.4. Podosoma and subcapitulum

The podosoma of *O. banksi* and *R. ardua* is essentially indistinguishable from that of *E. cooki*. Both the capitular apodeme and its lemniscus are identical in all three species.

#### 4.5 Conclusions

Ptychoidy is a complex mechanical defensive mechanism with a number of functional constraints for internal and external morphological features. For most exoskeletal characters, *R. ardua* and *E. cooki* are similar, as would be expected for confamilial species (Euphthiracaridae). We showed that *Oribotritia banksi*, a member of Oribotritiidae, differs from them in a number of exoskeletal characters. The internal functional morphology of ptychoidy, especially the arrangements of musculature and their attachment sites, remains to be compared for the three species. Further studies of ptychoidy in other families of the Ptyctima, as well as in groups of the Protoplophoridae and Mesoplophoridae, in combination with comparisons to non-ptychoid closely related outgroups, will help to differentiate between functional and phylogenetic constraints of ptychoidy.

## 5. Acknowledgements

We thank Karl-Heinz Hellmer for taking the SEM-micrographs. We thank Paavo Bergmann, Michael Laumann and Peter Cloetens for their help on the project SC-2127 at the ESRF in Grenoble. We thank the European Synchrotron Radiation Facility for the beam time.

## 6. References

- Alberti, G., R. A. Norton & J. Kasbohm (2001): Fine structure and mineralisation of cuticle in *Enarthronota* and *Lohmannioidea* (Acari: Oribatida). – In: Halliday, R. B., D. E. Walter, H. C. Proctor, R. A. Norton & M. J. Colloff (eds): *Acarology: Proceedings of the 10th International Congress*. – CSIRO Publishing, Melbourne: 230 – 241
- Balogh, J. & P. Balogh (1992): *The oribatid mites genera of the world, Vol. 1*. – Hungarian National Museum Press, Budapest: 263 pp.
- Betz, O., U. Wegst, D. Weide, M. Heethoff, L. Helfen, W.-K. Lee & P. Cloetens (2007): Imaging applications of synchrotron x-ray micro-tomography in biological morphology and biomaterial science. I. General aspects of the technique and its advantages in the analysis of arthropod structure. – *Journal of Microscopy* **22**: 51 – 71
- Grandjean, F. (1933): Structure de la region ventrale chez quelque Ptyctimina (Oribates). – *Bulletin du Muséum national d'Histoire naturelle* (2e ser) **5(A)**: 309 – 315
- Grandjean, F. (1934): Observations sur les Oribates (6e série). – *Bulletin du Muséum national d'Histoire naturelle* **6**: 353 – 360
- Grandjean, F. (1939): Observations sur les Oribates (11e série). – *Bulletin du Muséum national d'Histoire naturelle* **11**: 110 – 117
- Grandjean, F. (1954): Essai de classification des oribates. – *Bulletin de la Société Zoologique de France* **78**: 421 – 446
- Grandjean, F. (1967): Nouvelles observations sur les oribates (5e serie). – *Acarologia* **9**: 242 – 272
- Grandjean, F. (1969): Considerations sur le classement des oribates leur division en 6 groupes majeurs. – *Acarologia* **11**: 127 – 153
- Haumann, G. (1991): *Zur Phylogenie primitiver Oribatiden, Acari: Oribatida*. – dbv Verlag für die Technische Universität Graz, Graz: 237 pp.
- Mahunka, S. (1990): A survey of the superfamily Euphthiracaroidea Jacot, 1930 (Acari: Oribatida). – *Folia Entomology Hungary* **51**: 37 – 80
- Märkel, K. & I. Meyer (1959): Zur Systematik der deutschen Euphthiracarini (Acari, Oribatei). – *Zoologischer Anzeiger* **163**: 327 – 342
- Norton, R. A. (1984): Monophyletic groups in the *Enarthronota* (Sarcoptiformes). – In: Griffiths, D. A. & C. E. Bowman (eds): *Acarology VI, vol. I*. – Ellis Horwood, Chichester: 233 – 240
- Norton, R. A. (1994): Evolutionary aspects of oribatid mite life histories and consequences for the origin of the Astigmata. – In: Houck, M. (ed.): *Mites. Ecological and evolutionary analyses of life-history patterns*. – Chapman and Hall, New York: 99 – 135
- Norton, R. A. (2001): Systematic relationships of *Nothrolohmanniidae*, and the evolutionary plasticity of body form in *Enarthronota* (Acari: Oribatida). – In: Halliday, R. B., D. E. Walter, H. C. Proctor, R. A. Norton & M. J. Colloff (eds): *Acarology: Proceedings of the 10th International Congress*. – CSIRO Publishing, Melbourne: 58 – 75
- Norton, R. A. & V. Behan-Pelletier (1991): Calcium carbonate and calcium oxalate as cuticular hardening agents in oribatid mites (Acari: Oribatida). – *Canadian Journal of Zoology* **69**: 1504 – 1511

- Norton, R. A., F. H. Sanders & M. A. Minor (2003): *Euphthiracarus cooki* n. sp., a new oribatid mite (Acari: Oribatida) from Michigan and New York. – In: Smith, I. M. (ed.): An Acarological Tribute to David R. Cook – from Yankee Springs to Wheeny Creek. – Indira Publishing House, West Bloomfield: 201 – 210
- Rasputnig, G. (2006): Chemical alarm and defence in the oribatid mite *Collohmanna gigantea* (Acari: Oribatida). – *Experimental and Applied Acarology* **39**: 177 – 194
- Sanders, F. H. & R. A. Norton (2004): Anatomy and function of the ptychoid defensive mechanism in the mite *Euphthiracarus cooki* (Acari: Oribatida). – *Journal of Morphology* **259**: 119 – 154
- Saporito, R. A., M. A. Donnelly, R. A. Norton, H. M. Garraffo, T. F. Spande & J. W. Daly (2007): Oribatid mites as a major dietary source for alkaloids in poison frogs. – *Proceedings of the National Academy of Sciences* **104**: 8885 – 8890
- Schatz, H. (2002): Die Oribatidenliteratur und die beschriebenen Oribatidenarten (1758–2001) – eine Analyse. – *Abhandlungen und Berichte des Naturkundemuseums Görlitz* **74**: 37 – 45
- Shimano, S., T. Sakata, Y. Mizutani, Y. Kuwahara & J.-I. Aoki (2002): Geranial: The alarm pheromone in the nymphal stage of the oribatid mite, *Nothrus palustris*. – *Journal of Chemical Ecology* **28**: 1831 – 1837
- Subias, L. S. (2004): Listado sistemático, sinonímico y biogeográfico de los Ácaros Oribátidos (Acarifomes, Oribatida) del mundo (1748-2002). – *Graellsia* **60**: 3 – 305
- Travé, J., H.M. André, G. Taberly & F. Bernini (1996): Les Acariens Oribates. – In: Éditions AGAR and SIALF, Belgium
- Walker, N. A. (1965): Euphthiracaridae of California Sequoia litter, with a reclassification of the families and genera of the world. – *Fort Hayes Studies, Science Series* **3**: 1 – 155
- Wauthy, G., M. Leponce, N. Banaï, G. Sylin & J.-C. Lions (1998): The backward jump of a box moss mite. – *Proceedings of the Royal Society B* **265**: 2235 – 2242